Virus replication and competition in a cell culture: Application to the SARS-CoV-2 variants

L Ait Mahiout, Anastasia Mozokhina, A Tokarev, V Volpert

Version of Record: https://www.sciencedirect.com/science/article/pii/S0893965922001768
Manuscript_ac5549218cafe05c2ec65fc1d6853d7b

Virus replication and competition in a cell culture: application to the SARS-CoV-2 variants

L. Ait Mahiout[1a], A. Mozokhina[b], A. Tokarev[b,c], V. Volpert[d,b,*]

[a] *Laboratoire d'équations aux dérivées partielles non linéaires et histoire des mathématiques Ecole Normale Supérieure, B.P. 92, Vieux Kouba, 16050 Algiers, Algeria*
[b] *Peoples Friendship University of Russia (RUDN University), 6 Miklukho-Maklaya St, Moscow, 117198, Russia*
[c] *Semenov Institute of Chemical Physics RAS, Kosygin St., 4, 119991 Moscow, Russia*
[d] *Institut Camille Jordan, UMR 5208 CNRS, University Lyon 1, 69622 Villeurbanne, France*

Abstract

Viral replication in a cell culture is described by a delay reaction-diffusion system. It is shown that infection spreads in cell culture as a reaction-diffusion wave, for which the speed of propagation and viral load can be determined both analytically and numerically. Competition of two virus variants in the same cell culture is studied, and it is shown that the variant with larger individual wave speed out-competes another one, and eliminates it. This approach is applied to the Delta and Omicron variants of the SARS-CoV-2 infection in the cultures of human epithelial and lung cells, allowing characterization of infectivity and virulence of each variant, and their comparison.

Keywords: viral infection, virus competition, reaction-diffusion equations, SARS-CoV-2 variants
2010 MSC: 92C60, 92D30

1. Introduction

Viral infection spreads in a cell culture or in a tissue due to virus replication in the infected cells combined with virus diffusion in the extracellular space. This process is characterized by the spreading speed and by the viral load, that is, by the total quantity of virus in the culture at every moment of time. Both of them have important biological significance. Infection spreading speed *in vivo* determines the part of infected tissue and, as a consequence, the severity of related symptoms. Viral load in the upper respiratory tract in the case of respiratory infections determines virus infectivity, that is, the rate of infection transmission between individuals.

From the modelling point of view, viral infection spreading can be described as a reaction-diffusion wave [1, 2]. The wave speed and the viral load can be determined analytically through the model parameters, including the rate of cell infection and the rate of virus replication [3]. Analysis of the results show that spreading speed and viral load being determined by different

[1] Alphabetic order of authors
[*] Corresponding author
Email address: volpert@math.univ-lyon1.fr (V. Volpert)

combination of parameters may not correlate in the sense that for two viral infections, larger speed can be associated either with larger or smaller viral load.

Comparison of the time-dependent viral load with the experimental data on Delta and Omicron variants of the SARS-CoV-2 infection [4, 5] allow us to determine the parameters of the model and to use them to find the speed of infection spreading. These results have confirmed larger infectivity of the Omicron variant and weaker symptoms due to lung damage reported in the literature [8, 9]. Furthermore, we study the competition of two virus strains in a cell culture. We show that the virus with larger individual spreading speed wins this competition and eliminates another one independently of their relative viral loads. Noteworthy, these results are in agreement with the experimental data on the competition of Delta and Omicron variants in the cell cultures of human epithelial and lung cells [5].

2. Model of infection spreading

We describe the infection progression in a cell culture by the system of equations

$$\frac{\partial U}{\partial t} = -aUV, \quad \frac{\partial I}{\partial t} = aUV - \beta I, \quad \frac{\partial V}{\partial t} = D\frac{\partial^2 V}{\partial x^2} + bI_\tau - \sigma V \tag{2.1}$$

for the concentrations of uninfected cells U, infected cells I, and virus V [2]. The right-hand side of the first equation in (2.1) describes the rate of infection of uninfected cells, and there is a similar term in the second equation for infected cells. Influx and death of uninfected cells are not considered here since its influence are not essential in a short time scale. It will be taken into account in the subsequent works. The second term in the right-hand side of the second equation characterizes death of infected cells. The third equation in (2.1) describes virus random motion in the extracellular matrix (diffusion term), virus production in the infected cells with time delay in virus replication, $I_\tau(x,t) = I(x,t-\tau)$, and virus death (third term). In numerical simulations, we consider the system (2.1) on a bounded interval with no-flux boundary conditions for V, while in the analytical study we consider it on the whole axis.

2.1. Estimation of the wave speed and viral load

We are looking for the solution of system (2.1) in the form of reaction-diffusion wave: $U(x,t) = u(x-ct) = u(\xi), I(x,t) = w(x-ct) = w(\xi), V(x,t) = v(x-ct) = v(\xi)$, where all functions depend on the variable $\xi = x - ct$, c is the wave speed. System (2.1) becomes

$$cu' - auv = 0, \tag{2.2}$$

$$cw' + auv - \beta w = 0, \tag{2.3}$$

$$Dv'' + cv' + bw(\xi + c\tau) - \sigma v = 0. \tag{2.4}$$

We look for its solution on the whole real axis with the limits:

$$u(-\infty) = u_f, \; u(\infty) = u_0, \;\; v(\pm\infty) = w(\pm\infty) = 0 \tag{2.5}$$

(solution has zero derivatives at infinity). Here, constant u_0 is a given initial concentration of uninfected cells, while the final concentration of uninfected cells u_f is unknown. First, we will determine u_f, viral load and the wave speed c following the method from [2]. Then we will use them to construct the approximate analytical solution.

The final cell concentration and the total viral load. In order to determine the unknown value u_f, we derive the following equalities from equations (2.2)-(2.4) (cf. [2]):

$$c \ln \frac{u_0}{u_f} = a \int_{-\infty}^{\infty} v(x)dx, \quad c(u_0 - u_f) = \beta \int_{-\infty}^{\infty} w(x)dx, \quad b \int_{-\infty}^{\infty} w(x)dx = \sigma \int_{-\infty}^{\infty} v(x)dx. \quad (2.6)$$

Excluding the integrals from these equations, we obtain the equation

$$R_v(\omega - 1) = \ln \omega \quad (2.7)$$

with respect to $\omega = u_f/u_0$. Here, $R_v = abu_0/(\beta\sigma)$ is the virus replication number. Equation (2.7) has a solution ω in the interval $0 < \omega < 1$ if and only if $R_v > 1$. Consequently, if this condition is not satisfied, the problem (2.2)-(2.5) has no positive solution.

If $R_v > 1$, then the final value u_f can be found from equation (2.7), and the total viral load V_X defined as integral of $v(\xi)$ is given by the following formula:

$$V_X \equiv \int_{-\infty}^{\infty} v(x)dx = -\frac{c}{a} \ln \omega \, .$$

Furthermore, for R_v large enough, as it is the case of all virus variants of concern, solution ω of the equation (2.7) satisfies the estimate $\omega \ll 1$, and $\ln \omega \approx -R_v$. Therefore, $V_x \approx bcu_0/(\beta\sigma)$. Let us note that the viral load depends on the wave speed. We determine it below.

Wave speed. We approximate u by its value u_0 at $+\infty$. Therefore, we obtain the following linearized system of equations for w and v:

$$cw' + au_0 v - \beta w = 0, \quad (2.8)$$

$$Dv'' + cv' + bw(\xi + c\tau) - \sigma v = 0. \quad (2.9)$$

Let us look for the solution of this system in the form $w(\xi) = p_1 e^{-\lambda\xi}$, $v(\xi) = p_2 e^{-\lambda\xi}$. Substituting them into (2.8), (2.9), we obtain

$$-c\lambda p_1 + au_0 p_2 - \beta p_1 = 0,$$

$$D\lambda^2 p_2 - \lambda c p_2 + be^{-\lambda c\tau} p_1 - \sigma p_2 = 0.$$

In order to find the minimal wave speed, we should find the minimal value of c for which this system of equations has a positive solution λ. Introducing an independent parameter $\mu = \lambda c$ and excluding p_1 and p_2, we obtain the following equation:

$$D\frac{\mu^2}{c^2} - \mu + \frac{abu_0}{\mu + \beta} e^{-\mu\tau} - \sigma = 0.$$

Hence,

$$c = \min_{\mu > \mu_0} F(\mu) \equiv \frac{\sqrt{D}\mu}{\sqrt{\mu + \sigma - abu_0 e^{-\mu\tau}/(\mu + \beta)}} \, , \quad (2.10)$$

where μ_0 is a positive solution of the equation $(\mu + \sigma)(\mu + \beta) = abu_0 e^{-\mu\tau}$. This analytical formula for the minimal wave speed gives the same result as in numerical simulations (Figure 1, right).

2.2. Approximate analytical solution

We use the analytical expressions for the wave speed and viral load in order to construct an analytical approximation for the spatial distributions of virus and infected cell concentrations. Consider system (2.3), (2.4), where we approximate the function $u(\xi)$ by a piece-wise constant function corresponding to its limits at infinity: $u(\xi) = u_f$ for $\xi < 0$ and $u(\xi) = u_0$ for $\xi > 0$. For $\tau = 0$ this system can be solved analytically. Taking into account that the solution increases on the left half-plane, $u_f \approx 0$, and the solution decreases on the right half-plane, we get:

$$w = \begin{cases} p_3 e^{\frac{\beta}{c}\xi}, \ \xi < 0 \\ (p_1 + q_1\xi)e^{-\lambda\xi}, \ \xi > 0 \end{cases}, \quad v(\xi) = \begin{cases} p_4 e^{\lambda_1\xi} - \frac{bp_3}{D\beta^2/c^2+\beta-\sigma} e^{\frac{\beta}{c}\xi}, \ \xi < 0 \\ \left(\frac{c\lambda+\beta}{au_0}p_1 - \frac{c}{au_0}q_1 + \frac{c\lambda+\beta}{au_0}q_1\xi\right)e^{-\lambda\xi}, \ \xi > 0 \end{cases},$$

where λ is a positive double root of the characteristic equation for the system (2.8), (2.9) and

$$\lambda_1 = \frac{1}{2}\left(-\frac{c}{D} + \sqrt{\left(\frac{c}{D}\right)^2 + \frac{4\sigma}{D}}\right).$$

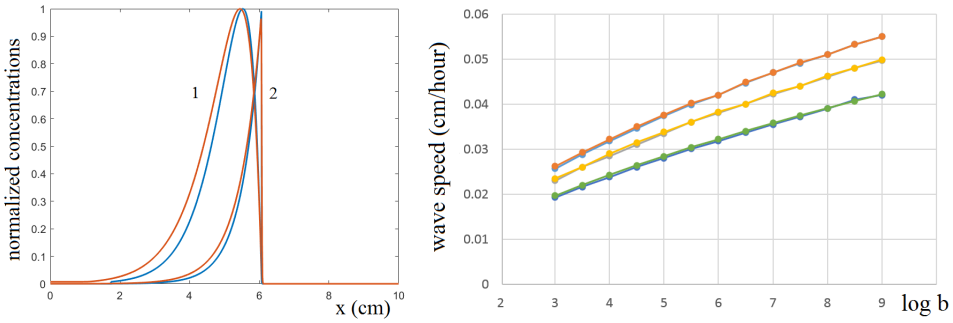

Figure 1: Left: virus concentration v (curve 1) and concentration of infected cells w (curve 2) in numerical simulations (red) and analytical approximation (blue) for the values of parameters: $a = 0.1$ $(1/(hour{\cdot}virus))$, $b = 1000$ $(copies/(hour{\cdot}cell))$, $\beta = 0.1$ $(1/hour)$, $\sigma = 0.1$ $(1/hour)$, $D = 10^{-4}$ $(cm^2/hour)$, $\tau = 0$ $(hour)$, and dimensionless concentrations $u_0 = 1, u_f = 0$. Analytical and numerical solutions for $v(\xi)$ are normalized by its maximum, $v_{max} = 3672$ $(copies/ml)$. Right: wave speed in numerical simulations and analytical formula (curves coincide) for the values of parameters: $a = 0.1, D = 0.001, \beta = 0, \sigma = 1, \tau = 2$ $(hour)$ (upper curve), $\tau = 5$ (middle curve) and $\tau = 8$ (lower curve). Note that the wave exists for $\beta = 0$, but viral load grows linearly in time [2].

Constants q_1, p_3, p_4 can be expressed through constant p_1 from continuity conditions $w(-0) = w(+0)$, $v(-0) = v(+0)$, and $v'(-0) = v'(+0)$, while constant p_1 can be found from the condition $\int_{-\infty}^{+\infty} v(\xi)\mathrm{d}\xi = -\frac{c}{a}\ln w$ (Appendix A). Altogether, this approach allows us to construct an approximate analytical solution (Figure 1, left).

3. Virus competition

In the case of two viruses (or virus variants) simultaneously present in cell culture, instead of system (2.1) we consider the system of equations:

$$\frac{\partial U}{\partial t} = -a_1 U V_1 - a_2 U V_2, \tag{3.1}$$

$$\frac{\partial I_1}{\partial t} = a_1 U V_1 - \beta_1 I_1, \qquad \frac{\partial I_2}{\partial t} = a_2 U V_2 - \beta_2 I_2, \tag{3.2}$$

$$\frac{\partial V_1}{\partial t} = D_1 \frac{\partial^2 V_1}{\partial x^2} + b_1 I_{1,\tau_1} - \sigma_1 V_1, \tag{3.3}$$

$$\frac{\partial V_2}{\partial t} = D_2 \frac{\partial^2 V_2}{\partial x^2} + b_2 I_{2,\tau_2} - \sigma_2 V_2. \tag{3.4}$$

Here V_1 and V_2 are virus concentrations, I_1 and I_2 are the concentrations of the corresponding infected cells. The meaning of all terms in these equations is similar to the one-virus model. As before, this system is considered on the whole axis in the analytical study, and in the bounded interval $0 \le x \le L$ with no-flux boundary conditions for the virus concentrations in the numerical simulations, and the initial condition $V_i(x,0) = V_0$ for $0 \le x \le x_0$ and 0 otherwise.

System (3.1)-(3.4) describes competition of two virus types for uninfected cells. If only the first virus is present initially, that is, $V_2(x,0) = 0$, then this is also true for all positive times, and this model is reduced to the previous one-virus model (2.1). Similarly, only the second virus type is observed if $V_1(x,0) = 0$. If both of them have positive concentrations at $t = 0$, then the result of their competition depends on the values of parameters. It can be formulated in the following form.

Proposition on virus competition. *Consider two virus types V_1 and V_2 and denote by c_1 and c_2, respectively, their individual propagation speeds in the one-virus model (2.1). Solution of the two-virus model (3.1)-(3.4) with positive initial conditions for both virus types converges to the one-virus solution $V_1(x,t)$ ($V_2(x,t)$) if and only if $c_1 > c_2$ ($c_1 < c_2$), while the concentration of another virus converges to 0 uniformly in $\mathbb{R}$. The two virus types coexist if and only if $c_1 = c_2$.*

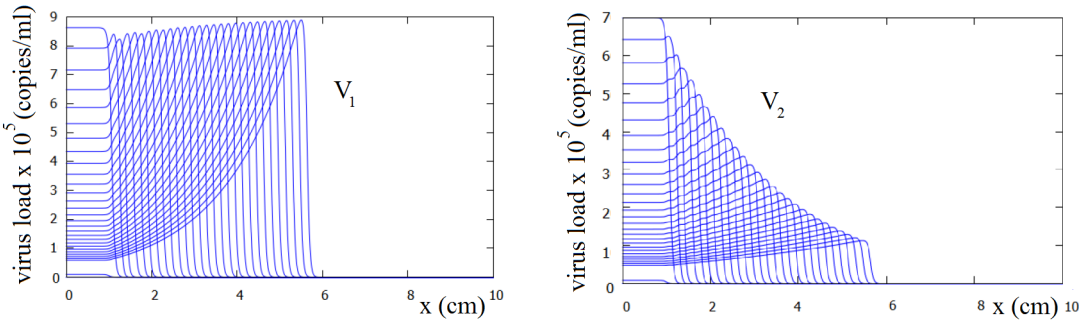

Figure 2: Numerical simulations of system (3.1)-(3.4) with the concentrations of the first virus in time (left) and the second virus (right). The individual wave speed of the first virus is larger since $a_1 b_1 > a_2 b_2$ (see (2.10)), and it eliminates the second virus, though the individual viral load of the second virus is larger. The values of parameters are as follows: $a_1 = 10^{-4}, a_2 = 10^{-5}, b_1 = 10^6, b_2 = 9 \cdot 10^6, D_1 = D_2 = 0.001, \sigma_1 = \sigma_2 = 1, \beta_1 = \beta_2 = 0.01, \tau_1 = \tau_2 = 10, L = 10, x_0 = 1, V_0 = 100$. Units of parameters are given in Figure 1.

This proposition is not proved mathematically since conventional methods of analysis and available results are not applicable here. We have verified this statement in numerical simulations for a large range of parameters. An example of numerical simulations is shown in Figure 2.

4. Competition of SARS-CoV-2 variants

We now apply the results on virus competition to Delta and Omicron variants of SARS-CoV-2 infection. We use the experimental data from [5] on time-dependent viral load for Delta and Omicron variants of the SARS-CoV-2 infection in cultures of human nasal cells (HNC) and human lung cells (HLC).

Comparison with the experimental data allows us to determine the parameters of the one-virus model for both variants and in the two types of cell culture (Figure 3). In the case of HNC, viral load for the Omicron variant is larger than that for the Delta variant in the beginning of the experiment, but it becomes less on days 2 and 3. However, the area under the curve (the integral of viral load) is larger for Omicron than for Delta. This is interpreted as an explanation of larger infectivity of Omicron variant [6]. Fitting the experimental data on the time-dependent viral load, as described in [2, 3], we determine the spreading speed for each variant. It is 0.0139 cm/hour for Delta and 0.0198 cm/hour for Omicron.

Comparison of numerical simulations with the experiments in the culture of lung cells is shown in Figure 3 (right). As before, we determine the parameters of the one-virus model and find the spreading speed. For Delta, speed is 0.0118 cm/hour, larger than the speed for Omicron, which is 0.0094 cm/hour.

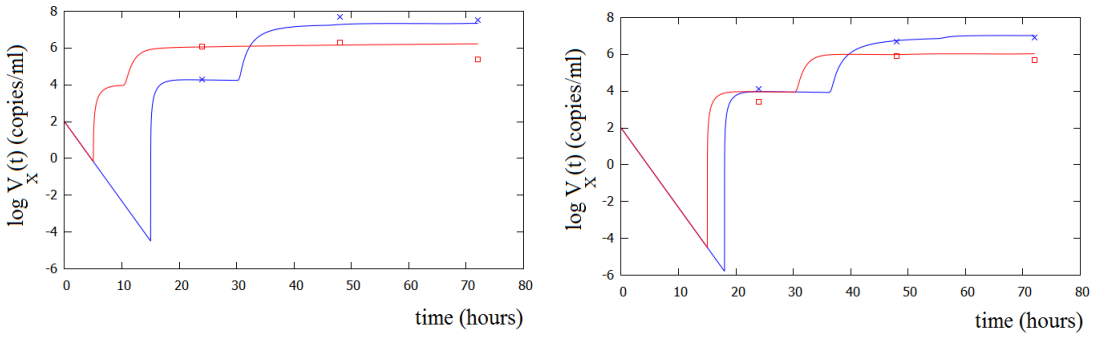

Figure 3: Left: human nasal cells, experimental results from [5] (dots) and numerical simulations with the values of parameters for Delta (blue): $a = 10^{-5}, b = 2 \cdot 10^7, \beta = 0.01, \sigma = 1, \tau = 15$; for Omicron (red): $a = 10^{-4}, b = 10^6, \beta = 0.01, \sigma = 1, \tau = 5$. Right: human lung cells, experimental results from [5] (dots) and numerical simulations with the values of parameters for Delta (blue): $a = 10^{-5}, b = 10^7, \beta = 0.01, \sigma = 1, \tau = 17$; for Omicron (red): $a = 10^{-4}, b = 10^6, \beta = 0.01, \sigma = 1, \tau = 15$. Common parameters: $D = 0.001, L = 10, x_0 = 1, v_0 = 100, u_0 = 1$. Units of parameters are given in Figure 1.

According to the analysis of the previous section, since the wave speed of the Omicron variant in the culture of HNC is larger than the wave speed of the Delta variant, then Omicron will eliminate Delta if both of them are introduced simultaneously. Next, since the relation between the wave speeds is opposite in the culture of lung cells, in this case Delta will eliminate Omicron. Both conclusions are confirmed by the numerical simulations, and they are in agreement with the experimental data [5].

5. Discussion

Viral infection in a cell culture or in a tissue can be characterized by the viral load and spatial spreading speed, which are different characteristics. For the respiratory infections, viral load in

the respiratory tract determines its infectivity, that is the rate of its transmission between individuals, while the spatial spreading speed correlates with the severity of symptoms for a given individual. Both quantities depend on cell (tissue) type as well as on viral variant. Available epidemiological data suggest that Omicron variant, compared to Delta, is more infectious [8], but its symptoms are weaker [9]. According to *in vitro* clinical data [6, 7], Omicron has larger viral load (area under the curve) in the upper respiratory tract than Delta, and vice versa in lungs (Figure 3, dots). However, these experiments are conducted in the homogeneous conditions, insensitive to spatial effects. Our numerical simulations were fitted to these clinical data (Figure 3, lines) but do include spatial effects, in particular diffusion limitation. These simulations suggest that Omicron variant, in addition to larger viral load, has larger spatial spreading speed in the upper respiratory tract than Delta variant. On the other hand, it has smaller spatial spreading speed in lungs.

Numerical simulations of the competition of two virus stains (Figure 2) affirm the proposition that virus with larger individual speed eliminates another one if both are introduced into the same cell culture to compete. This is a general conclusion for any two viruses competing for uninfected cells without other interaction between them (some coinfections can interact). This result corresponds to the experimental data for competing Delta and Omicron variants in the cultures of epithelial and lung cells [5].

One of the implications of this result concerns the emergence of the Omicron variant. Since it has a small spreading speed in the lungs, it is unlikely that it might appear due to mutations in the lungs of a single chronic COVID-19 patient (one of the existing hypothesis). It is more probable that it has emerged in the upper respiratory tract through a number of intermediate mutations in different individuals transmitting further these intermediate variants to other individuals.

Acknowledgements. The work has been supported by the RUDN University Strategic Academic Leadership Program.

References

[1] J. Yin, J. S. McCaskill Replication of viruses in a growing plaque: a reaction-diffusion model. Biophys. Journal, 61 (1992), 1540-1549.

[2] L. Ait Mahiout, N. Bessonov, B. Kazmierczak, G. Sadaka, V. Volpert. Infection spreading in cell culture as a reaction-diffusion wave. Mathematical Modelling and Numerical Analysis, 56 (2022) 791-814.

[3] L. Ait Mahiout, B. Kazmierczak, G. V. Volpert. Viral infection spreading and mutation in cell culture. Mathematics 2022, 10, 256. https://doi.org/10.3390/math10020256

[4] M. C. W. Chan et al. SARS-CoV-2 Omicron variant replication in human respiratory tract ex vivo. Biological Sciences. DOI: https://doi.org/10.21203/rs.3.rs-1189219/v1 Posted December 22, 2021.

[5] T. P. Peacock et al. The SARS-CoV-2 variant, Omicron, shows rapid replication in human primary nasal epithelial cultures and efficiently uses the endosomal route of entry. bioRxiv preprint doi: https://doi.org/10.1101/2021.12.31.474653 Posted January 3, 2022.

[6] A. Marc et al. Quantifying the relationship between SARS-CoV-2 viral load and infectiousness. eLife 2021;10:e69302. DOI: https://doi.org/10.7554/eLife.69302

[7] E. G. Bentley et al. SARS-CoV-2 Omicron-B.1.1.529 Variant leads to less severe disease than Pango B and Delta variants strains in a mouse model of severe COVID-19. bioRxiv preprint doi: https://doi.org/10.1101/2021.12.26.474085

[8] JRC Pulliam et al. Increased risk of SARS-CoV-2 reinfection associated with emergence of the Omicron variant in South Africa. medRxiv. 2 Dec 2021. https://doi.org/10.1101/2021.11.11.21266068

[9] V. Auvigne et al. Serious hospital events following symptomatic infection with Sars-CoV-2 Omicron and Delta variants: an exposed-unexposed cohort study in December 2021 from the COVID-19 surveillance databases in France. medRxiv preprint doi: https://doi.org/10.1101/2022.02.02.22269952

[10] F. Hecht, S. Auliac, O. Pironneau, J. Morice, A. Le Hyaric, K. Ohtsuka. FreeFEM++ (manual) www.freefem.org(2007)

Appendix A. Constants for the analytical solution

Constants p_1, q_1, p_3, and p_4 for the analytical solution from Section 2.2 are given by the following equalities:

$$p_1 = \frac{-c/a \ln w}{\frac{r_2}{\lambda_1} - \frac{b}{D\beta^2/c^2+\beta-\sigma} \cdot \frac{c}{\beta} + \frac{-c\lambda-\beta+cr}{-au_0\lambda} - \frac{-c\lambda-\beta}{au_0\lambda^2} r},$$

$$r = \frac{au_0 b(c\lambda_1 - \beta)}{c\left(D\beta^2/c^2 + \beta - \sigma\right)(c\lambda_1 + 2c\lambda + \beta)} - \frac{(-c\lambda - \beta)(\lambda_1 + \lambda)}{c\lambda_1 + 2c\lambda + \beta},$$

$$r_2 = \frac{b}{D\beta^2/c^2 + \beta - \sigma} - \frac{-c\lambda - \beta + cr}{au_0},$$

$$q_1 = rp_1, \; p_3 = p_1, \; p_4 = r_2 p_1.$$

Appendix B. Numerical implementation

The algorithm is based on explicit first order Euler scheme time-stepping procedure with $\mathbb{P}_1$ finite element spatial approximation where mesh size is equal to $L/10^4$. We use the free software FreeFEM [10] that offers a large variety of triangular finite elements (linear and quadratic Lagrangian elements, discontinuous P_1, Raviart-Thomas elements, etc) to solve partial differential equations. Numerical accuracy was controlled by decreasing time and space discretization and by the comparison with the analytical solution when it is available.

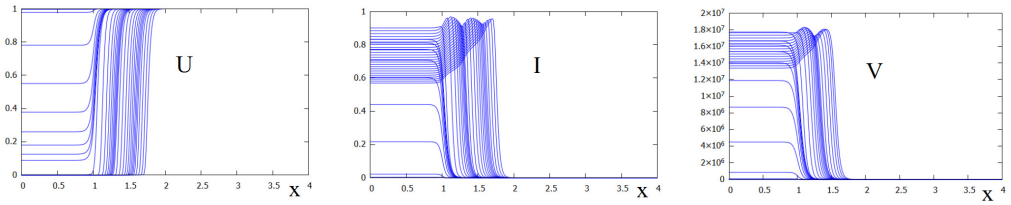

Figure B.4: Spatial distributions of uninfected cells U, infected cells I and virus V in consecutive moments of time as solution of system (2.1) for the same values of parameters as in Figure 3 (left, blue curve).

Numerical simulations in Figure B.4 show solution of system (2.1) for the same values of parameters as in Figure 3. Note that damped oscillations are related to time delay in the model (see also weak oscillations in Figure 3). Sensitivity of the results to parameters is determined by the analytical formulas for the viral load and wave speed.